JOURNAL OF MATERIALS SCIENCE **33** (1998) 5103–5110

Impedance spectroscopy of CuO-doped Y-TZP ceramics

C. BOWEN*
School of Materials, University of Leeds, Leeds LS2 9JT, UK

S. RAMESH†, C. GILL, S. LAWSON
School of Engineering & Advanced Technology, University of Sunderland, Sunderland, SR1 3SD, UK
E-mail: ramesh_singh@sirim.my

The effects of CuO additions on the grain interior and grain boundary resistivity in coated 2.5 mol % Y-TZP ceramics have been studied by using impedance spectroscopy. In addition, the effects of hydrothermal ageing on the conductivities of the ceramics were evaluated. The results showed that the grain interior and grain boundary resistivities increased with increasing CuO content. In particular, the grain boundary resistivity was observed to increase significantly in the doped ceramics, which could have been due to the formation of compounds, and resulted in lower conductivity. Impedance spectroscopy performed on the hydrothermally aged Y-TZPs revealed that the grain boundary regions were significantly affected, i.e. the grain boundary resistivities of the undoped and CuO-doped samples were increased by 65% and 45% respectively after ageing for 200 h. Thus, the indication is that the ageing-induced tetragonal to monoclinic phase transformation is closely associated with changes in the grain boundary regions.

1. Introduction

Impedance Spectroscopy (IS) is a relatively new and powerful means of characterising materials to provide information that is not accessible by electron microscopy alone. It may be employed to investigate mobile charges in the bulk or interfacial regions of any kind of solid or liquid e.g. ionic, semi-conducting and insulating [1].

There is considerable interest in zirconia materials due to their high oxygen ionic conductivity, which is required in applications such as oxygen sensors and solid oxide fuel cells [2]. Most high ionic conductivity research has concentrated on partially stabilised (PSZ) or fully stabilised cubic zirconia (FSZ). Yttria tetragonal zirconia polycrystalline ceramics (Y-TZP) have received some attention due to their high conductivities at moderate temperatures, combined with excellent mechanical properties [3, 4].

In Y-TZP ceramics, yttrium depletion of grain boundaries or at the external surface has been observed by various workers [5–10] to have an effect on the resistivity and ionic conductivity of the material. Since the grain boundaries in polycrystalline ceramic materials often have a large impact on the properties of the material, detailed knowledge of grain boundary behaviour is essential for the optimisation of material properties. It is for this reason that impedance spectroscopy is an important tool for the characterisation of zirconia ceramics. Bauerle [11] was the first to introduce impedance spectroscopy as a technique for the determination of conductivity in zirconia materials.

At moderate temperatures ($<600\,^{\circ}C$) the grain interior of Y-TZP has a lower resistivity when compared to fully or partially stabilised zirconia [12]. However, some Y-TZP materials have higher overall ionic resistivities due to a continuous grain boundary glassy phase which increases the grain boundary resistivity [13]. The grain boundary resistivity in FSZ is often reduced by increasing the grain size of the material (the grain boundary area per unit volume is decreased) or by producing "easy paths" for conduction (no continuous grain boundary phase). For Y-TZP, an increase in grain size is less desirable as it leads to destabilisation of the material [14] which decreases the ionic conductivity and is deleterious to the mechanical properties due to the formation of the monoclinic phase. However, a lowering of grain boundary resistivity in Y-TZP can be achieved by decreasing the level of impurities which segregate at grain boundaries or by altering the composition of the grain boundary [15].

A limitation of Y-TZP ceramics is the undesirable surface tetragonal to monoclinic phase transformation during ageing at low temperatures ($60\,^{\circ}C$–$500\,^{\circ}C$) in humid environments [16]. The grain boundary region

Current address:
* Department of Materials Science and Engineering, University of Bath, Bath, BA2 7AY, UK.
† Ceramics Technology Laboratory, SIRIM BERHAD, 1 Persiaran Dato Menteri, P.O. Box 7035, Section 2, 40911 Shah Alam, Malaysia.

is thought to play an important part in determining the hydrothermal or corrosive degradation of zirconia. Therefore, additives (such as CuO [17, 18]) are often used to change the grain boundary composition. As IS can determine grain interior and boundary properties it is a powerful tool in examining the effect of dopants and ageing in Y-TZP.

The aim of this work was to examine the effects of CuO additions on the grain interior and boundary properties of Y-TZP ceramics. In addition, the effects of hydrothermal ageing on the electrical conductivity of the materials were also evaluated.

2. Experimental

Commercially available 2.5 mol % yttria co-coated zirconia powders (2.5Y-TZP) supplied by Tioxide Specialties Ltd., UK., were prepared by synthesis of ZrO_2 in a plasma reactor, rapid cooling and coating with yttria in a process described elsewhere [19]. The as-received 2.5Y-TZP powder had a total impurity concentration of about 1.7 wt %, with 0.08 wt % Al_2O_3 and 1.6 wt % HfO_2 as the major impurities. Varying amounts of CuO (0.05, 0.2 and 1 wt %) were mixed with the 2.5Y-TZP powder matrices by a wet-milling technique [20]. Disc samples were made by uniaxial pressing at 35 MPa followed by cold isostatic pressing at 200 MPa. All the samples were sintered at 1300 °C for 2 hours at a ramp rate of 10 °C/min. The sintered samples were polished on one face to a 1 μm surface finish prior to testing.

Densities of the samples were measured using a water immersion method. Phase analysis by X-ray diffraction of polished samples was carried out at room temperature using CuK_α as the radiation source. The fraction of surface monoclinic content was evaluated using the method of Toraya *et al*. [21]. Microstructural evolution was examined by scanning electron microscopy (SEM). The grain size was determined on thermally etched specimens from scanning electron micrographs using the line intercept analysis of Mendelson [22]. Complex electrical impedance measurements were made on pellets 14 mm diameter and 3 mm thick which had Pt electrodes fired on to each surface. Impedance measurements were carried out in the frequency range 0.1 Hz to 500 kHz using a Solatron 1260 Frequency Response Analyser at temperatures of 250, 275, 300, 330, 360, 400 and 450 °C.

The resistive and capacitive components of the grain interior (R_{gi} and C_{gi}) and grain boundary (R_{gb} and C_{gb}) were extracted from the impedance spectra using an equivalent circuit as proposed by Bauerle [11] (see Fig. 1). Resistance measurements were converted to resistivity values by normalising with respect to sample size [1].

Selected samples were hydrothermally aged at 180 °C and 1 MPa for 200 hours and tested to examine ageing effects on the grain interior and grain boundary properties.

3. Results and discussion

3.1. Properties of as-sintered samples

In Table I, the measured room temperature properties of the samples are presented. The results clearly shows the beneficial effects of incorporating small amounts (0.05 and 0.2 wt %) of CuO in 2.5Y-TZP ceramics. These doped samples exhibited higher bulk densities (>6 Mgm^{-3}) and finer grain sizes if compared to the undoped ceramics.

In contrast, the 1 wt % CuO doped material could not be tested accurately as the large amount of monoclinic (m) zirconia present in the sample induced cracking in the material.

TABLE I Room temperature properties of as-sintered (1300 °C) Y-TZPs

CuO content	Tetragonal content (%)	Bulk density (Mgm^{-3})	Ave. grain size (μm)
0 wt % (undoped)	97	5.91	0.16
0.05 wt %	98	6.03	0.13
0.20 wt %	98	6.03	0.15
1.0 wt %[a]	~ 20	~ 4.86	Porous structure

[a]Surface cracks were evident after sintering.

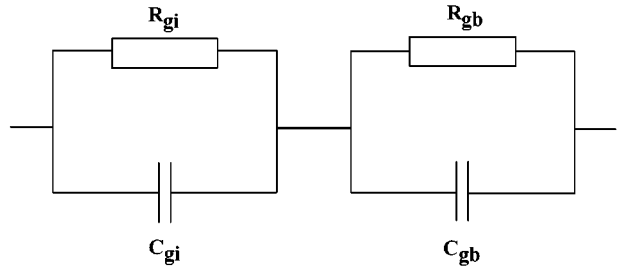

Figure 1 Equivalent circuit used to interpret impedance spectroscopy results (After Bauerle [11]).

3.2. Effects of CuO on resistivity

It was found that in the temperature range 250 to 450 °C, the grain interior and grain boundary resistivities were clearly resolved in the impedance spectrum as there was a large enough difference in the time constants of the regions. Typical experimental complex impedance spectra obtained for samples tested at 330 °C are shown in Fig. 2.

It can be observed from Fig. 2, that as the frequency was reduced, these plots show a small grain interior arc, a large grain boundary arc and part of an electrode arc which extends below the frequency range employed. The existence of the electrode arc in all of the samples suggests that the conductivity was essentially ionic [3].

The results in Fig. 2 also clearly indicate that the resistivities of the Y-TZP were significantly affected by the additions of CuO. Relative to the CuO-doped samples, the undoped ceramics (profile 1) had a lower grain interior resistivity (ρ_{gi}) and grain boundary resistivity (ρ_{gb}), hence an overall lower total resistivity, see Table II.

In the doped samples, the resistivity values were found to increase with CuO content. The relatively high total resistivity of the 0.2 wt % CuO-doped sample as indicated in Table II was mainly due to the high grain boundary resistivity. Similar results were obtained for the range of temperatures employed in

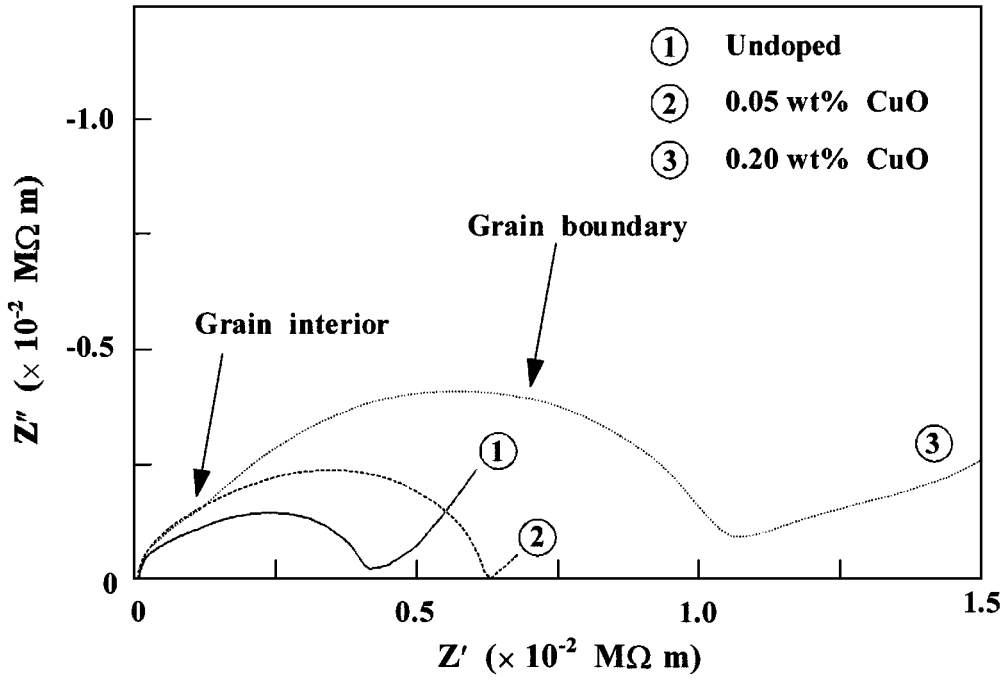

Figure 2 Complex impedance plot for undoped and CuO-doped Y-TZPs measured at 330 °C. Similar trends were noted throughout the temperature range investigated.

TABLE II A comparison of the resistivity values for grain interiors (ρ_{gi}), grain boundaries (ρ_{gb}) and total resistivity (ρ_t) for Y-TZPs measured at 330 °C

Y_2O_3 content (mol %)	CuO content (wt %)	Resistivity ($\times 10^3\ \Omega$ m)		
		ρ_{gi}	ρ_{gb}	ρ_t
2.5	0	1.2	2.6	3.8
2.5	0.05	1.5	4.3	5.8
2.5	0.20	1.9	8.1	10.0

the present work. In general, the high resistivity of the CuO-doped samples, in particular for grain boundaries as indicated by the impedance spectra confirmed the existence of a resistive grain boundary phase, which was CuO-rich. Moreover, the grain size in these samples was small (<0.15 μm) resulting from low temperature sintering. Thus the grain boundary length was much higher and combined with the presence of CuO, could have accounted for the higher grain boundary resistivity.

In order to obtain the activation energies for grain interior and grain boundary conduction, the equation for the ionic conductivity usually applied to a doped oxide conductor is given by [23]:

$$\sigma T = A_\sigma \exp\left[\frac{-\Delta H_\sigma}{kT}\right] \quad (1)$$

where, σ = conductivity of the material at temperature T (Ω^{-1} m^{-1}), ΔH_σ = activation energy for conduction (eV), T = temperature (K), k = Boltzmann's constant (eV K^{-1}) and A_σ = pre-exponential factor (KΩ^{-1} m^{-1}). The process enthalpy (ΔH_σ) usually contains the true activation energy for charge migration as well as associate energy terms for defect formation [23].

The Arrhenius plots of $\ln(\rho/T)$ versus $(1/T)$ for ρ_{gi} and ρ_{gb} were constructed as shown in Fig. 3. In addition, calculated values of A_σ and ΔH_σ, respectively, in the present work and those reported by Bonanos *et al.* [3, 24] for TZP, PSZ and FSZ are compared in Table III.

It has been found that the activation energies for grain interior and grain boundaries in the present Y-TZPs showed a small increase with increasing CuO additions, see Table III. However, in general the calculated activation energies for conduction of grain boundaries

TABLE III Calculated parameters for the conductivity equations for the grain interiors and grain boundaries of Y-TZPs in the present work. The corresponding values for Y-TZP, Y-PSZ and Y-FSZ reported by Bonanos *et al.* [3] are also included for comparison purposes

Sample	Pre-exponential ($\times 10^2\ \Omega^{-1}$ m^{-1} K)		Activation energies (eV)	
	A_{gi}	A_{gb}	$\Delta H_{\sigma gi}$	$\Delta H_{\sigma gb}$
Undoped 2.5Y-TZP	3.8×10^6	7.7×10^6	1.06	1.14
0.05 wt % CuO-doped	2.8×10^6	5.1×10^6	1.06	1.14
0.20 wt % CuO-doped	2.6×10^6	4.3×10^6	1.07	1.17
3 mol % Y-TZP [3]	5.5×10^5	3.7×10^6	0.92	1.09
4.7 mol % Y-PSZ [3]	6.1×10^6	6.8×10^7	1.07	1.15
6 mol % Y-FSZ [3]	6.8×10^6	5.2×10^7	1.07	1.12

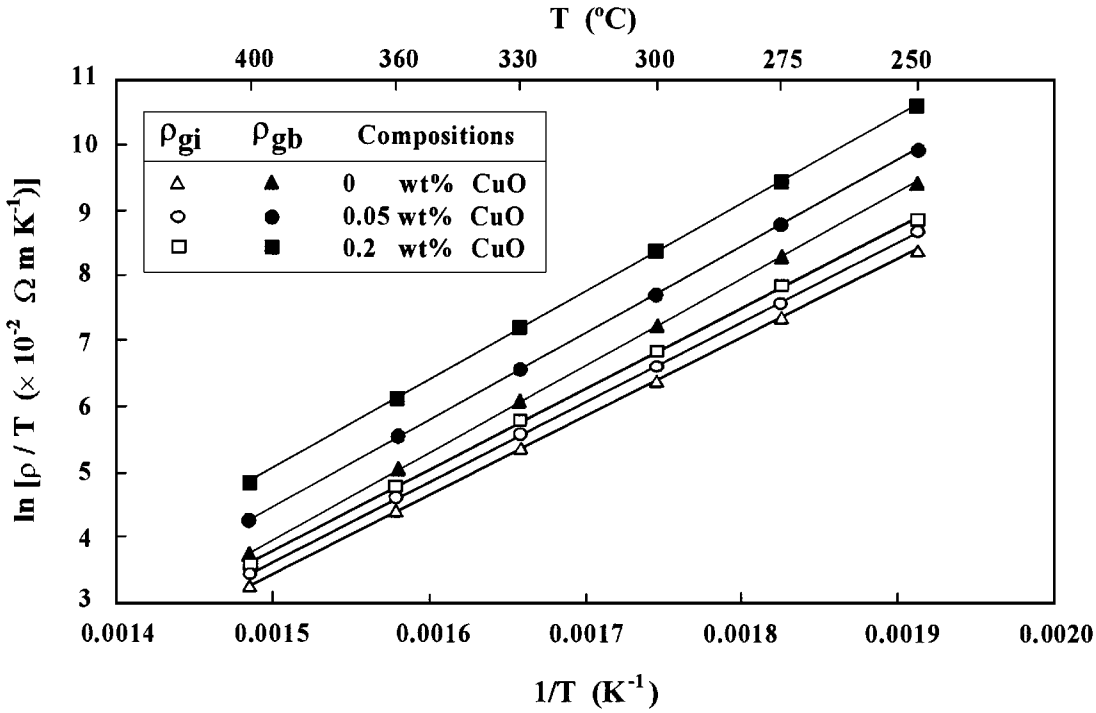

Figure 3 Arrhenius plots of the grain interior and grain boundary resistivity for undoped and CuO-doped Y-TZPs. Note that ρ_{gi} and ρ_{gb} increases with increasing CuO content.

are higher than that of the grain interior. These results are in agreement with those reported in literature for TZP ceramics [3, 25, 26].

The fact that the activation energies for grain interior and grain boundary are consistently different implies that the "brick layer" model [27, 28] is appropriate for this material, i.e. the material has a *continuous* and homogeneous grain boundary phase layer with a much higher specific resistivity than that of the bulk material [11, 24, 29].

A comparison of the activation energies results obtained in the present Y-TZPs with those reported by Bonanos *et al.*, in Table III, reveals some differences. In all cases, the calculated values for $\Delta H_{\sigma gi}$ and $\Delta H_{\sigma gb}$ in the present work were slightly higher than those reported by Bonanos *et al.* for Y-TZP. This discrepancy in results could be attributed to the differences in processing conditions, compositions, yttria content and distribution, sintering conditions and the resultant microstructure [30].

As in the work of Bonanos *et al.* [24] and Jurado *et al.* [25], the pre-exponential factors for grain interior conductivity in the present Y-TZP ceramics were lower than that in PSZ of FSZ although the activation energies of all these ceramics were almost similar, see Table III.

In general, the higher ionic conductivities in TZP ceramics reported in literature are related to the lower activation energy for conduction [25, 31]. Bonanos *et al.* [24] explained that in doped fluorite oxides such as ZrO_2, the oxygen vacancies are trapped by the dopant cations hence reducing the free vacancy concentration. Therefore the activation enthalpy for conduction, ΔH_σ, in Y^{3+} doped ZrO_2, is the sum of the true activation enthalpy of migration ΔH_m and the enthalpy of association ΔH_a due to defect formation (i.e. $\Delta H_\sigma = \Delta H_m + \Delta H_a$). Both, the enthalpy of migration and association can vary depending on cation type and size [23]. For instance it has been reported that the values of ΔH_m and ΔH_a in FSZ are 0.6 to 0.7 eV and 0.4 to 0.5 eV respectively [23, 32], thus giving ΔH_σ of approximately 1.1 eV.

However, in many cases it is difficult to ascertain which of these parameters, ΔH_m and ΔH_a, vary with changing compositions. Badwal and Swain [31] found that the enthalpy of migration ΔH_m is more sensitive than the enthalpy of association ΔH_a, i.e. ΔH_m increases significantly with yttria content.

In the present work, from the temperature range investigated both the activation energies $\Delta H_{\sigma gi}$ and $\Delta H_{\sigma gb}$ of the undoped coated 2.5 mol % Y-TZP and both the CuO-doped samples were almost similar (see Table III). Therefore, it can be assumed that the introduction of CuO in Y-TZP did not cause additional lattice defects (i.e. oxygen vacancies) in the ZrO_2 lattice but rather altered the grain boundary phase making it more resistant to charge transport resulting in lower conductivity. Although more in-depth studies are required to understand these results, it can be inferred that the processing technique of the present Y-TZP powder, resulting in an inhomogeneous yttria distribution (i.e. higher yttria concentrations near grain boundary regions [19]) was responsible for the results obtained.

3.3. Specific grain boundary resistivity (ρ_{sp}) and grain boundary thickness (δ_{gb})

In the present work an attempt was also made to determine the grain boundary thickness of the Y-TZPs from the impedance data. Table II shows that as the CuO content increased, the resistivity of the grain boundary region increased significantly. However, the undoped and CuO-doped Y-TZPs had different grain sizes and

TABLE IV Specific grain boundary resistivity (ρ_{sp}) as a function of temperature

Temperature (°C)	Specific grain boundary resistivity, ρ_{sp} ($\times 10^{-4}\ \Omega\,m^2$)		
	0 wt % CuO	0.05 wt % CuO	0.20 wt % CuO
250	156.76	137.40	318.10
275	52.61	45.80	104.37
300	19.17	16.79	36.95
330	6.40	5.63	12.17
360	2.35	2.08	4.39
400	0.67	0.61	1.27

the grain boundary resistivity is affected by impurity segregation at the grain boundaries and the size of the grain. Therefore, to compare the effect of grain sizes on the resistivity, the value of ρ_{gb} was corrected for grain size. This was achieved by determining the grain boundary resistivity per unit surface area (ρ_{sp}) [33]:

$$\rho_{sp} = R_{gb} \cdot \left[\frac{A}{t}\right] \cdot D_g = \rho_{gb} \cdot D_g \qquad (2)$$

where, D_g = grain size, A = sample surface area and t = thickness of the material. The results are presented in Table IV.

It can be seen from Table IV, that when the grain size of the material was considered the value of ρ_{sp} for the 0.05 wt % CuO-doped sample was not significantly altered if compared to the undoped Y-TZP for the range of temperatures investigated. However, as the CuO content increased to 0.20 wt % a larger value of ρ_{sp} was observed. This increase in ρ_{sp} could be attributed to higher amounts of CuO segregated at grain boundary regions.

The difference in activation energies (ΔH_{gb} and ΔH_{gi}) (see Table III) implies a continuous grain boundary phase is present in the ceramics. For the "brick layer" tetragonal ceramics, the grain boundary capacitance may be used to calculate the grain boundary thickness (δ_{gb}) [11, 27, 28]:

$$\delta_{gb} = \varepsilon_0 \varepsilon_r \frac{D_g}{C_{gb}} \cdot \frac{A}{t} \qquad (3)$$

where ε_0 = electric constant or permittivity of free space, ε_r = relative permittivity of the grain boundary phase, and C_{gb} = grain boundary capacitance (F).

One of the major difficulties in using this equation to calculate grain boundary thickness is to determine the appropriate value for the relative permittivity of the grain boundary phase, ε_r, since the composition of this phase differs considerably from one powder to another and is dependent on the quantity and type of impurities present. Several authors have reported an ε_r value of 22 to 30 [34, 35] for stabilised zirconia while others had considered a higher value, e.g. 70 [36]. However in the present work $\varepsilon_r = 30$ has been applied. Table V shows the outcome of the calculations for the three materials investigated. For the undoped Y-TZP a grain boundary thickness of 2 nm has been calculated which agrees well with published work on other Y-TZPs [27, 37–40].

TABLE V Estimated grain boundary thickness (δ_{gb}) for Y-TZPs

Composition	0 wt % CuO	0.05 wt % CuO	0.20 wt % CuO
C_{gb}(F m^{-1})	3.05×10^{-8}	2.30×10^{-8}	2.86×10^{-8}
ε_r	30	30	30
D_g ($\times 10^{-6}$ m)	0.24	0.13	0.15
δ_{gb} ($\times 10^{-9}$ m)	2.08	1.50	1.40

In contrast, the additions of CuO to Y-TZP ceramics resulted in a decrease in grain boundary thickness, see Table V. The grain boundary thicknesses of both the 0.05 wt % and 0.2 wt % CuO-doped ceramics were found to be similar. This is in fact in agreement with the initial results on sintering which showed no significant change in properties with increasing CuO content up to 0.2 wt % [20]. It should be noted, however, that these measurements assume that the grain boundary permittivity remained constant as CuO was added to the Y-TZP. Therefore, an accurate comparison of δ_{gb} as a function of CuO content is difficult as the grain boundary composition was different for each material. The calculation of smaller δ_{gb} values for the copper oxide doped samples is surprising as it was anticipated that more grain boundary glassy phase would be present when the dopant concentration was higher.

3.4. Effects of hydrothermal ageing on resistivity of CuO-doped Y-TZPs

In order to confirm the speculation that during ageing monoclinic phase nucleates near grain boundary regions, impedance spectroscopy (IS) was employed to investigate the changes in resistivity of the hydrothermally aged samples (180 °C and 1 MPa, after 200 h exposure). The results obtained for grain interior, ρ_{gi} and grain boundary resistivity, ρ_{gb} of the aged samples were compared with those of the unaged samples. Fig. 4 shows the impedance spectra comparing the unaged and hydrothermally aged materials.

As shown in Fig. 5, the least ageing resistant material was the undoped Y-TZP and the most ageing resistant material was the 0.05 wt % CuO-doped Y-TZP. The greatest change in the spectra occurred in the undoped Y-TZP (see Fig. 4) while the CuO-doped materials exhibited the lowest changes, which was consistent with the fact that small additions of CuO enhanced the ageing resistance.

3.4.1. Grain interior resistivity changes

The percentage changes in grain interior resistivities measured at 330 °C for the aged samples when compared to the unaged Y-TZPs are presented in Table VI.

A large change in grain interior resistivity was observed for the undoped Y-TZP, which was due to the formation of a (m)-ZrO_2 layer on the surface of the sample after the ageing test (i.e. the m-layer thickness measured was 750 μm for 200 h ageing). In contrast, for the CuO-doped Y-TZPs, no significant changes in ρ_{gi} was observed. These results correlate well with the detection of small amounts of surface (m) phase content

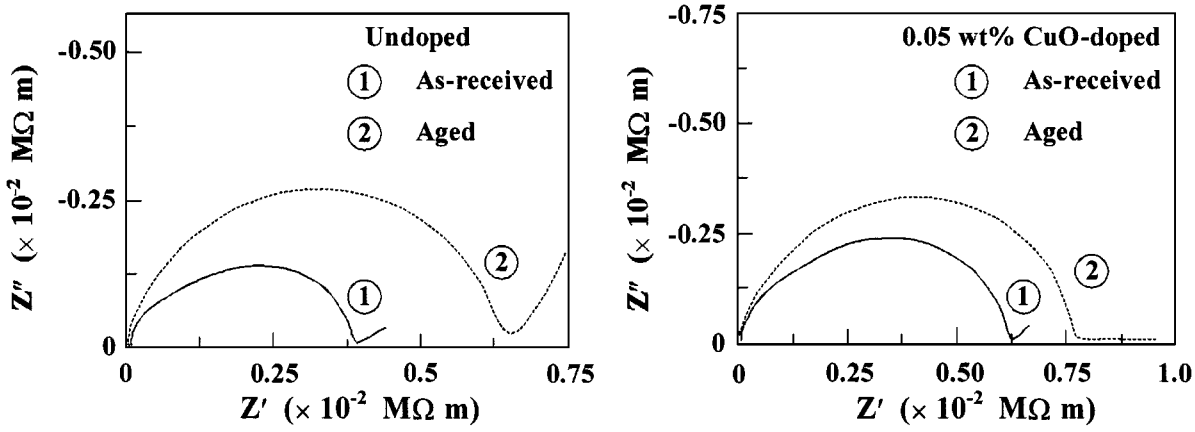

Figure 4 Comparison of the impedance spectra of the as-received and hydrothermally aged (180 °C and 1 MPa, 200 h) Y-TZPs.

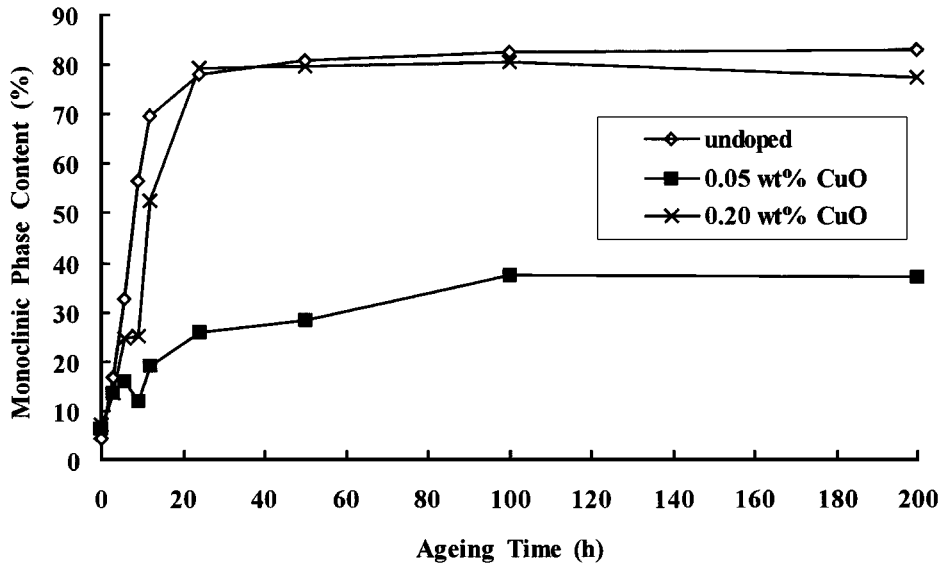

Figure 5 The effects of CuO additions on the ageing behaviour (180 °C and 1 MPa) of Y-TZPs.

TABLE VI Change in grain interior (ρ_{gi}) and specific grain boundary (ρ_{sp}) resistivity measured at 330 °C for the aged Y-TZPs

	Undoped Y-TZP	0.05 wt % CuO-doped
$\Delta\rho_{gi}$	+48%	−3%
$\Delta\rho_{sp}$	+65%	+45%

Note: $+ve$ = an increase and $-ve$ = a decrease.

using the XRD method and microscopic examination of the transformed layer thickness e.g. 4 μm after 200 h ageing of the 0.05 wt % CuO-doped sample.

3.4.2. Specific grain boundary resistivity changes

The grain boundary area is thought to play an important role in governing the ageing of Y-TZP ceramics. This is indicated by the large changes in the specific grain boundary resistivity (ρ_{sp}) of the aged materials shown in Table VI. It can be observed that the introduction of CuO in Y-TZP decreases the change in ρ_{sp}. The largest change of ρ_{sp} was observed in the undoped Y-TZP, which was the least ageing resistant material. On the other hand, an increase of over 40% in ρ_{sp} was also observed in the 0.05 wt % CuO-doped sample, which was unusual as there were no significant changes in grain interior resistivity, see Table VI. This increase in ρ_{sp} could have been due to some development of monoclinic phase adjacent to grain boundaries or a reaction in the boundary. This large increase indicates that even though the aged (m)-layer layer in this sample is of the order of a few microns after ageing, the grain boundary regions seemed to be greatly affected.

Therefore, based on these results, it can be concluded that during ageing (m) nucleation initiated near grain boundaries, which in turn explained the increase in ρ_{sp} observed for the 0.05 wt % CuO-doped sample. No significant change in ρ_{gi} was observed in the 0.05 wt % CuO doped sample which suggests that the presence of CuO at the grain boundaries had retarded the propagation of monoclinic phase to grain interior by preventing the formation of either Zr–OH or Y–OH bonds. This was confirmed by the extreme slow (m) layer propagation rate as indicated in Fig. 6 for the 0.05 wt % CuO-doped sample i.e. the addition of 0.05 wt % CuO was effective in retarding the (m) layer propagation rate by a factor of more than 300 as shown in parentheses in Fig. 6.

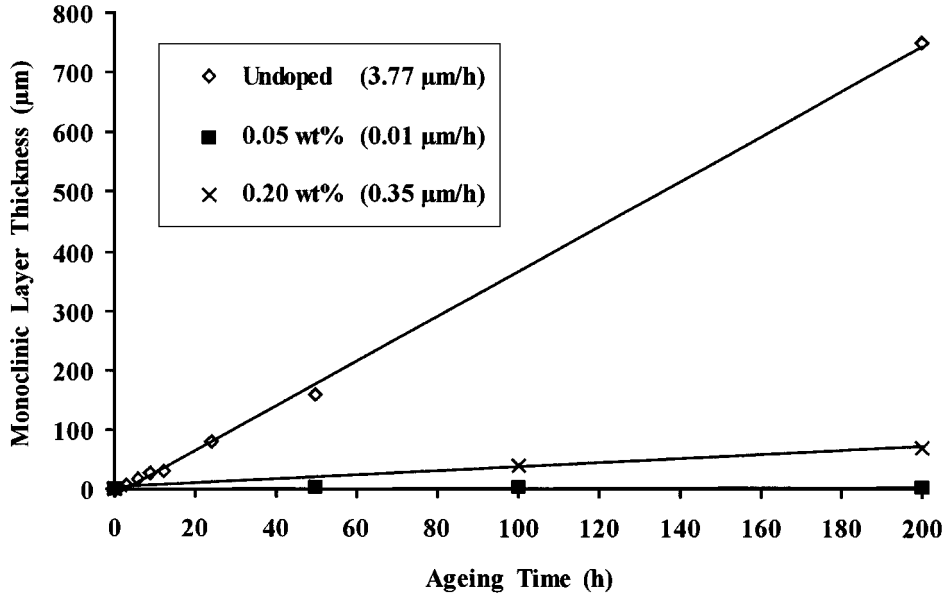

Figure 6 The effects of ageing (superheated steam, 180 °C and 1 MPa) on the (m) layer propagation rate.

4. Conclusions

1. Impedance spectroscopy has been used to estimate the effects of CuO additions and of ageing on coated 2.5 mol % Y-TZP ceramics.

2. The grain interior resistivity decreased with increasing CuO content. This may have been due to grain interior yttria dissolution into the CuO glassy phase along the grain boundaries. Activation energies for grain interior conduction are similar and agree with other reported data on Y-TZP.

3. Calculated grain boundary thicknesses for the undoped Y-TZP was approximately 2 nm which is consistent with other observations on high purity Y-TZP materials.

4. The specific grain interior resistivity decreased when 0.05 wt % CuO is added to Y-TZP, which was possibly due to the decrease in grain size so that impurities were segregated over a wider area. This correlated with the observed decrease in the grain boundary thickness.

5. The highest specific grain boundary resistivity and smallest grain boundary thickness were observed in the 0.20 wt % CuO-doped sample. An increase in the intrinsic grain boundary resistivity or errors in assuming a constant grain boundary permittivity with large CuO contents may explain this discrepancy.

6. The consistent difference in grain interior and grain boundary activation energies implies that the brick layer model is appropriate for this material.

7. After hydrothermal ageing, the grain interior resistivity increased for the undoped Y-TZP. This is due to the formation of a large monoclinic layer which has lower ionic conduction. For the CuO-doped materials, no significant change in ρ_{gi} was observed indicating the enhanced ageing resistance of CuO-doped Y-TZP.

8. An increase in the grain boundary resistivity was observed in the undoped and 0.05 wt % CuO-doped Y-TZPs after treating in superheated steam for 200 h. This phenomenon was also attributed to the formation of monoclinic phase adjacent to grain boundaries.

9. Since, there was no significant change in grain interior resistivity as compared to the specific grain boundary resistivity in the CuO-doped Y-TZP, it can be inferred that grain boundary regions are active sites for monoclinic nucleation during ageing.

Acknowledgements

The authors thank Tioxide Specialties Ltd. and in particular, Dr. G. P. Dransfield, for supplying the starting powders used in this study and the support of the School of Engineering and Advanced Technology at the University of Sunderland UK. Dr. Ramesh Singh gratefully acknowledges SIRIM BERHAD and the Malaysian Government for the financial support.

References

1. J. R. MacDONALD and W. B. JOHNSON, in "Fundamentals of Impedance Spectroscopy—Impedance Spectroscopy: Emphasizing Solid Materials and Systems," edited by J. R. MacDonald (John Wiley & Sons, Inc., 1987) p. 1.
2. B. C. H. STEELE, J. DRENNAN, R. K. SLOTWINSKI, N. BONANOS and E. P. BUTLER, in "Advances in Ceramics: Science and Technology of Zirconia," Vol. 3, edited by A. H. Heuer and L. W. Hobbs (American Ceramic Society, Inc., Columbus, Ohio, 1981) p. 286.
3. N. BONANOS, R. K. SLOTWINSKI, B. C. H. STEELE and E. P. BUTLER, *J. Mater. Sci. Letts.* **3** (1984) 245.
4. K. KEIZER, M. VAN HEMERT, A. J. A. WINNUBST, M. A. C. G. VAN DE GRAAF AND A. J. BURGGRAAF, *J. De Physique.* **47** (1986) C1-783.
5. M. M. R. BOUTZ, A. J. A. WINNUBST and A. J. BURGGRAAF, *J. Eur. Ceram. Soc.* **13** (1994) 89.
6. S. P. S. BADWAL, *J. Mater. Sci. Letts.* **6** (1987) 1419.
7. A. E. HUGHES and B. A. SEXTON, *ibid.* **24** (1989) 1057.
8. A. E. HUGHES and S. P. S. BADWAL, *Solid State Ionics* **46** (1991) 265.
9. E. P. BUTLER, R. K. SLOTWINSKI, N. BONANOS, J. DRENNAN and B. C. H. STEELE, in "Advances in Ceramics: Science and Technology of Zirconia II," Vol. 12, edited by N. Claussen, M. Ruhle and A. H. Heuer (American Ceramic Society, Columbus, Ohio, 1984) p. 572.
10. J. DRENNAN and S. P. S. BADWAL, in "Advances in Ceramics: Science and Technology of Zirconia III," Vol. 24B, edited

by S. Somiya, N. Yamamoto and H. Yanagida (American Ceramic Society, Inc. Westerville, Ohio, 1988) p. 807.
11. J. E. BAUERLE, *J. Phys. Chem. Solids.* **30** (1969) 2657.
12. S. P. S. BADWAL and J. DRENNAN, *J. Mater. Sci.* **24** (1989) 88.
13. S. P. S. BADWAL and A. E. HUGHES, *J. Eur. Ceram. Soc.* **10** (1992) 115.
14. T. K. GUPTA, *Science of Sintering* **10** (1978) 205.
15. J. DRENNAN and E. P. BUTLER, *Sci. of Ceram.* **12** (1983) 267.
16. S. LAWSON, *J. Eur. Ceram. Soc.* **15** (1995) 485.
17. S. RAMESH, C. GILL, S. LAWSON and G. P. DRANSFIELD, Presented at the Pacific Rim 2, International Ceramic Conference, Australia 1996, Paper No. 555.
18. S. LAWSON, C. GILL and G. P. DRANSFIELD, *J. Mater. Sci.* **30** (1995) 3057.
19. G. P. DRANSFIELD, in "Engineering Ceramics: Fabrication Science and Technology," *Brit. Ceram. Proc.*, No. 50, edited by D. P. Thompson (The Institute of Materials, London, 1993) p. 1.
20. S. RAMESH, Ph.D. thesis, University of Sunderland, UK, 1997.
21. H. TORAYA, M. YOSHIMURA and S. SOMIYA, *J. Am. Ceram. Soc.* **67** (1984) C-119.
22. M. I. MENDELSON, *ibid.* **52** (1969) 443.
23. J. A. KLINER and R. J. BROOK, *Solid State Ionics* **6** (1982) 237.
24. N. BONANOS, B. C. H. STEELE, E. P. BUTLER, W. B. JOHNSON, W. L. WORRELL, D. D. MACDONALD and M. C. H. MCKUBRE, in "Impedance Spectroscopy: Emphasising Solid Materials and Systems," edited by J. R. MacDonald (John Wiley & Sons, Inc., 1987) p. 191.
25. J. R. JURADO, C. MOURE and P. DURAN, *J. de Phys. Coll.* **47** (1986) C1-789.
26. M. J. VERKERK, A. J. A. WINNUBST and A. J. BURGGRAAF, *J. Mater. Sci.* **17** (1982) 3113.
27. M. GODICKEMEIER, B. MICHEL, A. ORLIUKAS, P. BOHAC, K. SASAKI, L. GAUCKLER, H. HEINRICH, P. SCHWANDER, G. KOSTORZ, H. HOFMANN and O. FREI, *J. Mater. Res.* **9** (1994) 1228.
28. M. J. VERKERK, B. J. MIDDELHUIS and A. J. BURGGRAAF, *Solid State Ionics* **6** (1982) 159.
29. S. P. S. BADWAL and J. DRENNAN, *J. Mater. Sci.* **22** (1987) 3231.
30. S. RAMESH, C. GILL, S. LAWSON and G. P. DRANSFIELD, *ibid.* **31** (1996) 6055.
31. S. P. S. BADWAL and M. V. SWAIN, *J. Mater. Sci. Letts.* **4** (1985) 487.
32. J. E. BAUERLE and J. HRIZO, *J. Phys. Chem. Solids* **30** (1969) 565.
33. M. KUWABARA, T. MURAKAMI, M. ASHIZUKA, Y. KUBOTA and T. TSUKIDATE, *J. Mater. Sci. Letts.* **4** (1985) 467.
34. R. MORRELL, in "Handbook of Properties of Technical and Engineering Ceramics—Part 1: An Introduction for the Engineer and Designer" (National Physics Laboratory, London, 1989) p. 162.
35. C. BOWEN, Private Communication, University of Leeds, UK. (1996).
36. T. VAN DIJK and A. J. BURGGRAAF, *Phys. Stat. Sol. (a)* **63** (1981) 229.
37. M. RUHLE, M. L. MECARTNEY and N. CLAUSSEN, in "Ceramic Materials and Components for Engines," edited by W. Bunk and H. Hausner (American Ceramic Society, Columbus, Ohio, 1986) p. 593.
38. H. SCHUBERT, N. CLAUSSEN and M. RUHLE, in "Advances in Ceramics: Science and Technology of Zirconia II," Vol. 12, edited by N. Claussen, M. Ruhle and A. H. Heuer (American Ceramic Society, Columbus, Ohio, 1984) p. 766.
39. T. STOTO, M. NAUER and C. CARRY, *J. Am. Ceram. Soc.* **74** (1991) 2615.
40. M. RUHLE, N. CLAUSSEN and A. H. HEUER, in "Advances in Ceramics: Science and Technology of Zirconia II," Vol. 12, edited by N. Claussen, M. Ruhle and A. H. Heuer (American Ceramic Society, Columbus, Ohio, 1984) p. 352.

Received 20 August
and accepted 14 September 1998